

Article

Utilizing Date Palm Leaf Biochar for Simultaneous Adsorption of Pb(II) and Iodine from Aqueous Solutions

Essam R. I. Mahmoud ^{1,*}, Hesham M. Aly ², Noura A. Hassan ³, Abdulrahman Aljabri ¹, Asim Laeeq Khan ⁴ and Hashem F. El-Labban ⁵

¹ Department of Mechanical Engineering, Faculty of Engineering, Islamic University of Madinah, Madinah 42351, Saudi Arabia; aaljabri@iu.edu.sa

² Department of Forestry and Timber Trees, Horticulture Research Institute, Agricultural Research Center, Antoniadis Botanical Garden, Alexandria 21554, Egypt

³ Pesticide Chemistry & Technology Department, Faculty of Agriculture, Alexandria University, Alexandria 21545, Egypt

⁴ Department of Chemical Engineering, Faculty of Engineering, Islamic University of Madinah, Madinah 42351, Saudi Arabia; akhan@iu.edu.sa

⁵ Production Engineering Department, Faculty of Engineering, Alexandria University, Alexandria 21545, Egypt

* Correspondence: essamibrahim2@yahoo.com

Abstract: This study addresses the environmental and health hazards posed by Pb(II) and iodine, two significant contaminants. The objective was to explore the adsorption of these substances from aqueous solutions using biochar derived from the leaf midribs of the date palm through a slow pyrolysis process. The pyrolysis was conducted in two stages within a vacuum furnace: initially at 300 °C for 1 h followed by overnight cooling, and then at 600 °C with a similar cooling process. The resulting biochar was characterized for its microstructural features and functional groups using scanning electron microscopy (SEM) and Fourier transform infrared (FT-IR) spectroscopy. It exhibited a porous structure with large numbers of pores (20 to 50 μm in size) and functional groups including O-H, C-H, and C=C, which are integral to its adsorption capabilities. For the adsorption studies, a 100 ppm Pb(II) ion solution was treated with varying amounts of biochar (20, 40, 60, and 80 mg) for 24 h. In parallel, iodine adsorption was tested, with biochar quantities ranging from 0.1 to 0.4 g/50 mL. Both treatments were followed by filtration and analysis using atomic absorption spectroscopy to determine the remaining concentrations of Pb(II) and iodine. The study also explored the effect of varying incubation periods (up to 30 h) on iodine adsorption. The results were significant; 100% adsorption of Pb(II) was achieved with the addition of 60 mg of biochar per 10 mL of solution. In contrast, for iodine, a maximum adsorption of 39.7% was observed with 30 mg or 40 mg of biochar per 50 mL. These findings demonstrate the potential of date palm-derived biochar as an effective and sustainable material for the removal of Pb(II) and iodine from contaminated water, offering valuable insights for environmental remediation strategies.

Keywords: biochar; adsorption; lead ion; iodine; pyrolysis



Citation: Mahmoud, E.R.I.; Aly, H.M.; Hassan, N.A.; Aljabri, A.; Khan, A.L.; El-Labban, H.F. Utilizing Date Palm Leaf Biochar for Simultaneous Adsorption of Pb(II) and Iodine from Aqueous Solutions. *Processes* **2024**, *12*, 1370. <https://doi.org/10.3390/pr12071370>

Academic Editors: Titus Chinedu Egbosiuba and Chinenye Adaobi Igwegbe

Received: 27 May 2024

Revised: 25 June 2024

Accepted: 28 June 2024

Published: 1 July 2024



Copyright: © 2024 by the authors. Licensee MDPI, Basel, Switzerland. This article is an open access article distributed under the terms and conditions of the Creative Commons Attribution (CC BY) license (<https://creativecommons.org/licenses/by/4.0/>).

1. Introduction

The environmental and health implications of toxic heavy metals, particularly lead (Pb), are profound and multifaceted. Pb, originating from a variety of industrial processes such as battery production, tetraethyl manufacturing, refining, and automobile maintenance, is a harmful pollutant [1]. Its toxicity poses severe risks to human health, including detrimental effects on the kidney, stomach, and nervous system [2]. Moreover, lead contamination is not limited to industrial sites; it extends to water bodies and soils, exacerbated by natural processes and anthropogenic activities [3]. This widespread contamination highlights the urgent need for effective remediation strategies.

The methods employed to remove Pb from wastewater are diverse, ranging from ion exchange and membrane processes to chemical precipitation, filtration, electrocoagulation, coagulation, and adsorption [1]. Among these, adsorption is often preferred for its cost-effectiveness, simplicity, and high efficiency. The performance of the adsorption process is significantly influenced by the properties of the adsorbent material used. In this context, biochar, produced from biomass via pyrolysis, has emerged as a sustainable and efficient solution. The quality of biochar, in terms of its adsorption capacity and overall properties, is largely determined by the type of feedstock and the conditions under which pyrolysis is conducted [4,5].

Biochar's effectiveness as an adsorbent is attributed to its highly porous structure, substantial specific surface area, cation exchange capacity, and abundance of surface functional groups [1]. These attributes make biochar particularly suitable for the adsorption of heavy metals like Pb. Studies have demonstrated the successful application of biochar derived from various biomass sources, including pinewood and rice husk, in the adsorption of lead from water [6]. Biochar derived from the date palm have been studied as adsorbents for heavy metals from wastewater by different investigators such as those described in the review of [7,8]. The bio-adsorbent prepared from date pits is efficient in the adsorption of heavy metals from aqueous solutions [8]. In the study of Alghamdi et al. [9], biochar was prepared from date palm waste and magnetized through Fe-intercalation. The prepared biochar before and after magnetization were used to absorb Cd(II) and Pb(II) ions from water. The adsorption capacity in the case of magnetic biochar is higher than that in case of biochar. However, the two materials showed higher removal of Pb(II) as compared with Cd(II) [9]. In another study, palm fibers were chemically modified by sulfuric acid, oxalic acid as a chelating agent, HNO₃ as an oxidizing agent, and Na₂SO₃ as a reducing agent [10]. The highest capacity of adsorption for both Pb(II) and Cd(II) ions has been obtained in the case of palm fibers which were modified by sulfuric acid. Also, palm fibers modified by oxidizing agents gave good results [10]. Biochar was produced from date seed biomass and used for the adsorption of lead ions (Pb(II)) from an aqueous solution [11]. The best adsorption conditions were obtained by preparing the biochar at 550 °C with a heating time of 3 h. The maximum adsorption capacity was found to occur at a pH of nearly 6.0. The health of humans is negatively affected by the excess levels of NO₃ in drinking water [12]. Biochar was produced from palm leaf residues at a pyrolyzing temperature of 600 °C and different pH, and used for the adsorption of nitrate from the solution [12]. The most adsorption of nitrate from the solution (90%) was obtained at pH 2 [12].

Expanding the scope of biochar use, researchers have also explored its potential in adsorbing heavy metals from wastewater using biochar derived from date palms. Date pits, for instance, have been processed into bio-adsorbents showing considerable efficiency in removing heavy metals from aqueous solutions [13,14]. In a novel approach, date palm-waste biochar was magnetized through Fe-intercalation, enhancing its capacity to adsorb Cd(II) and Pb(II) ions [15]. Additionally, chemical modifications of palm fibers with various agents have led to improved adsorption capacities for Pb(II) and Cd(II) ions [16].

Beyond heavy metals, the environmental contamination with iodine, specifically the isotopes I131 and I129 from nuclear power plants, poses a significant health hazard due to their radioactive effects [17,18]. The contamination of the environment with iodine can also be resulted from food, chemical and pharmaceutical industries [19]. Due to the high toxicity of iodine to the thyroid glands, and the occurrence of hypothyroidism that resulted from excessive amounts of iodine, its removal from the environment is necessary [20]. To remove the iodine from aqueous solutions, some adsorbents such as activated carbon, metal-exchanged zeolite, porous copper-doped silica zeolites, graphene, aerogel, metalorganic frameworks, and porous organic polymer materials were used [21]. The metalorganic frameworks showed high absorptivity, but they are unsuitable [18]. Cyclodextrin is a non-toxic and biodegradable material. It is a representative of cyclic oligosaccharide macromolecules [22]. Cyclodextrin (CD) derivatives (α , β , γ and β -hydroxypropyl-CD) were successfully immobilized on a silica gel surface via epichlorohydrin as a cross-linker [23].

It is expected that I₂ molecules can be adsorbed on the hydrophobic chains and in CD hydrophobic cavities [24]. The best performance in the adsorption of iodine from aqueous solutions has been obtained in the case of functionalized silica with β -hydroxypropyl-CD [23].

Methods for iodine removal have also included the use of activated carbon, metal-exchanged zeolite, and, more recently, metalorganic frameworks and cyclodextrin immobilized on silica gel [20,21]. The latter has shown promising results in adsorbing iodine from aqueous solutions [21]. To adsorb iodine from an aqueous solution, low-cost biochar was prepared from empty oil palm bunches by the application of a hydrothermal carbonation process [25]. The biochar was activated before and after pyrolysis by heating it using an autoclave at 121 °C for 90 min. The pre- and post-treatments, applied in the production of these biochar, could increase the surface area and the adsorption capacity of the produced biochar [26]. In these treatments, alkaline activators were used. Biochar was then soaked using NaOH or KOH with a concentration of 0%, 4%, 8%, and 12% for 3 h. The results showed that the adsorption of iodine ranged from 208.86–616.32 mg/g [25,26].

This study addresses the critical need for effective removal of both Pb(II) and iodine from aqueous solutions. We propose a novel approach utilizing biochar produced from the leaf midribs of the date palm. This research not only investigates the potential of date palm waste as a sustainable resource for biochar production, but also explores the impact of biochar concentrations and incubation periods on the adsorption of these contaminants. By doing so, the study seeks to offer a low-cost, efficient, and environmentally friendly solution to mitigate the adverse effects of Pb(II) and iodine contamination, thereby contributing significantly to the field of environmental remediation and public health.

The novelty of this research lies in its dual focus on sustainable resource utilization and environmental protection for Pb and iodine removal from wastewater. By converting agricultural waste into a valuable adsorbent, this study not only addresses waste management issues but also provides a viable method for purifying contaminated water sources. Moreover, this is one of the few studies that simultaneously targets the removal of both Pb(II) and iodine using biochar derived from date palm leaves, which has not been extensively explored in the existing literature. The comprehensive analysis of biochar's structural properties and its interaction with contaminants offers deep insights into the mechanisms of adsorption, paving the way for future advancements in biochar technology and its application in environmental remediation.

2. Materials and Methods

2.1. Biochar Preparation

The method for preparing biochar, as detailed in our previous work [27], involves a two-step pyrolysis process using the leaf midribs of the date palm. This procedure was specifically designed to optimize the properties of the biochar for adsorption purposes.

Initially, the date palm leaf midrib samples were subjected to air drying for a duration of four weeks. This step ensures the removal of moisture, which is crucial for the efficiency of the pyrolysis process. Following the drying phase, the samples were placed in a vacuum furnace for pyrolysis.

The pyrolysis process was carried out in two distinct stages.

In the first stage, the dried samples were gradually heated to a temperature of 300 °C at a controlled rate of 10 °C per minute. Upon reaching 300 °C, the samples were maintained at this temperature for a period of 1 h. This stage is critical for initiating the pyrolysis process and beginning the transformation of the biomass into biochar. After the completion of the first stage, the samples were allowed to cool down to room temperature overnight. This gradual cooling is an essential step in the process, as it affects the final structure and composition of the biochar. In the second stage of pyrolysis, the specimens were reheated at the same rate of 10 °C per minute until they reached 600 °C. Once at 600 °C, the samples were held at this temperature for another hour. This higher temperature stage further advances the pyrolysis process, contributing to the development of the biochar's porous

structure and enhancing its adsorption properties. Following this, a second cooling phase was carried out, where the specimens were again allowed to cool throughout the night.

This two-step pyrolysis process is specifically tailored to enhance the adsorptive qualities of the biochar, particularly for the removal of Pb(II) and iodine from aqueous solutions. The controlled heating and cooling cycles play a pivotal role in determining the physical and chemical characteristics of the resulting biochar, making it suitable for environmental remediation applications.

2.2. Biochar Characterization

To comprehensively characterize the surface features of the produced biochar, we utilized scanning electron microscopy (SEM) (Jeol JSM-5300 SEM) equipped with an electron dispersive X-ray (EDX) analysis unit. This combination of techniques allowed us to closely examine the microstructural properties and elemental composition of the biochar surface, providing critical insights into its morphological and chemical characteristics.

Further analysis of the biochar was conducted using Fourier transform infrared (FT-IR) spectroscopy in the range of 400–4000 cm^{-1} . This technique was instrumental in identifying and mapping the distribution of functional groups on the biochar surface, which are key determinants of its adsorption capabilities.

2.3. Adsorption Studies

To evaluate the biochar's efficiency in adsorbing Pb(II) ions, we prepared a standard solution of 100 ppm Pb(II) ions. A quantity of 1.6 g of $\text{Pb}(\text{NO}_3)_2$ was dissolved in 1.0 L of deionized water to produce 5.0 mM Pb(II) stock solution for which the initial pH was adjusted as needed using 0.1 M NaOH and 0.1 M HCl to obtain pH 6. Various amounts of biochar (20, 40, 60, and 80 mg) were incubated with this solution for 24 h. Post-incubation, the solutions were filtered using a syringe filter with a 0.2 μm pore size. The residual concentrations of Pb(II) ions were then quantified using atomic absorption spectroscopy, based on a pre-established calibration curve. The percentage of adsorption (%Ads) was calculated using the equation below:

$$\% \text{ Ads} = \frac{\text{Conc. in control} - \text{conc. in treatment}}{\text{Conc. in control}} \times 100 \quad (1)$$

In a parallel set of experiments, we prepared a 0.1 M standard iodine solution in 1 L of distilled water as a stock solution. To quantify iodine, a standard solution of 0.1 N Na_2SO_3 was prepared for titration in the presence of a starch indicator, proceeding until the color disappeared. Different amounts of biochar (0.1, 0.2, 0.3, and 0.4 g) were incubated with 50 mL of the iodine solution for 1 h, then filtered with a 0.2 μm syringe filter. The residual iodine concentration was determined post-filtration.

Additionally, to investigate the effect of incubation time on the adsorption of iodine by palm tree biochar, the amount of biochar yielding the best adsorption results was incubated with a 50 mL iodine solution for varying periods (2, 4, 8, 12, 24, and 30 h). The solutions were then filtered and the residual iodine concentration was measured using the 0.1 N Na_2SO_3 standard solution.

3. Results and Discussion

3.1. Biochar Characterization before and after Pb(II) Adsorption

The SEM analysis of the biochar surface before Pb(II) adsorption presented in Figure 1 reveals its microstructural characteristics at two different zones. The observed porous structure, characterized by lateral and anterior vessels, is a key feature of the biochar. This structure comprises a large number of pores, predominantly in the size range of 20 to 50 μm . These findings are in line with previous studies that have reported similar microstructural properties in biochar produced under comparable conditions [5,7,9–11]. The porous nature of the biochar is critical for its adsorption capabilities, as it provides an extensive surface area for interaction with contaminants.

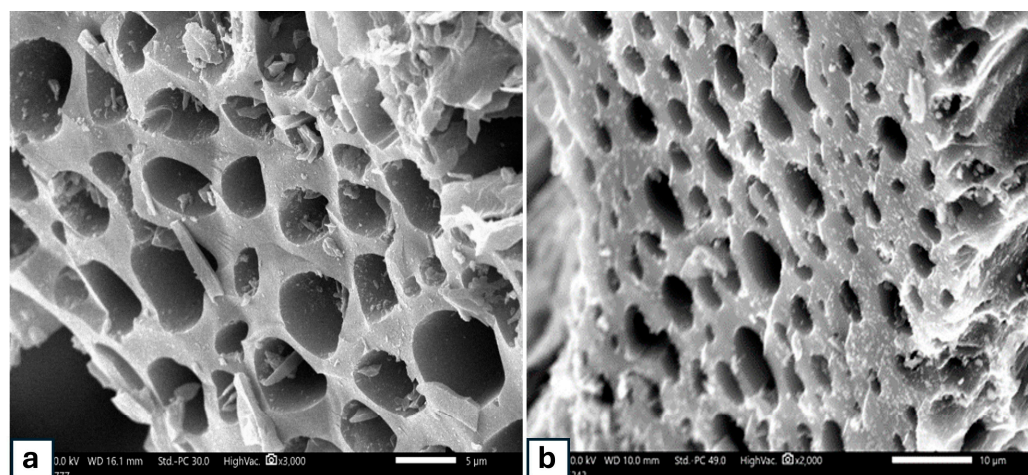
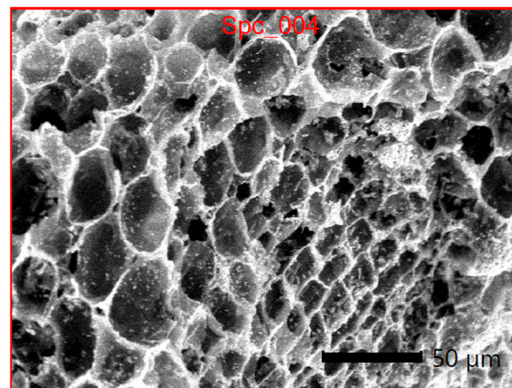


Figure 1. SEM images of the microstructure of the biochar surface at two different zones: (a) anterior vessels, and (b) lateral vessels.

In Figure 2, the EDX analysis image of the biochar after Pb(II) adsorption is shown, highlighting a specific section marked with a red circle. This analysis reveals the elemental composition of the biochar, where carbon, oxygen, and lead are identified as the predominant elements. The high carbon content, a result of the pyrolysis process, is indicative of the transformation of organic matter into a carbon-rich material. The presence of carbon (C) and oxygen (O) in significant amounts suggests the formation of various functional groups, such as C=C (carbon–carbon double bonds) and C–O (carbon–oxygen bonds), which are crucial for the adsorption process. The integration of these results—the microstructure observed through SEM and the elemental composition determined by EDX—provides a comprehensive understanding of the biochar’s properties. The porous microstructure enhances the surface area available for adsorption, while the presence of specific functional groups contributes to the chemical interactions necessary for effective contaminant removal.

In our analysis of the biochar surface before Pb(II) adsorption using FT-IR spectroscopy, as shown in Figure 3, we identified a range of functional groups integral to the biochar’s adsorptive characteristics. The observed stretching vibrations of the O–H group, notably in the range of $3220\text{--}3743\text{ cm}^{-1}$ [28], are associated with hydrogen-bonded O–H groups commonly found in carboxylic and phenolic compounds. These functional groups are crucial in the biochar’s ability to form hydrogen bonds, a key interaction in the adsorption process. Moreover, the presence of C–H (methyl) groups, observed in the range of $2850\text{--}2920\text{--}3039\text{ cm}^{-1}$ [29], suggests aliphatic substitution on aromatic rings. This structural feature enhances the hydrophobic nature of the biochar, facilitating the adsorption of non-polar substances. The peak detected around 1570 cm^{-1} , indicating the ring stretching of C=C [30], further confirms the presence of aromatic compounds. This characteristic is essential for the biochar’s $\pi\text{--}\pi$ interactions, contributing to its high adsorptive capacity. Aliphatic C–H groups, evidenced by bands at 1420 cm^{-1} [31], add another layer of complexity to the biochar’s chemical structure. Additionally, peaks in the range of 1112 cm^{-1} , corresponding to stretching C–O groups in phenolic compounds, alcoholic compounds, and carboxylic acids [28], underscore the biochar’s ability to adsorb metal ions due to its polar nature. The biochar’s lignocellulosic origin is reflected in the observed O–H hydrogen bonds and C–H bonds, typically derived from cellulose, and the C=C bonds resulting from lignin aromatic rings [32]. The presence of these components implies that the biochar retains structural elements from its biomass precursor, enhancing its adsorption properties. C=O bonds, indicative of carboxylic or carbonyl groups [33], play a vital role in the biochar’s capacity to chelate metal ions. This functionality is particularly relevant for heavy metal adsorption. Furthermore, the presence of inorganic matter, as suggested by bands in the range of $468\text{--}615\text{ cm}^{-1}$ [34], such as carbonates, can influence the biochar’s overall

adsorption capacity. Finally, the C-H aromatic out-of-plane bands [35] suggest a high degree of aromaticity, a feature that contributes to the biochar's adsorptive performance.



Display name	Standard data	Quantification method	Result Type
Spc_004	Standardless	ZAF	Metal
Element	Line	Mass%	Atom%
C	K	61.29±0.63	82.74±0.84
O	K	15.21±0.84	15.42±0.85
Pb	M	23.50±0.88	1.84±0.07
Total		100.00	100.00
Spc_004			Fitting ratio 0.2248

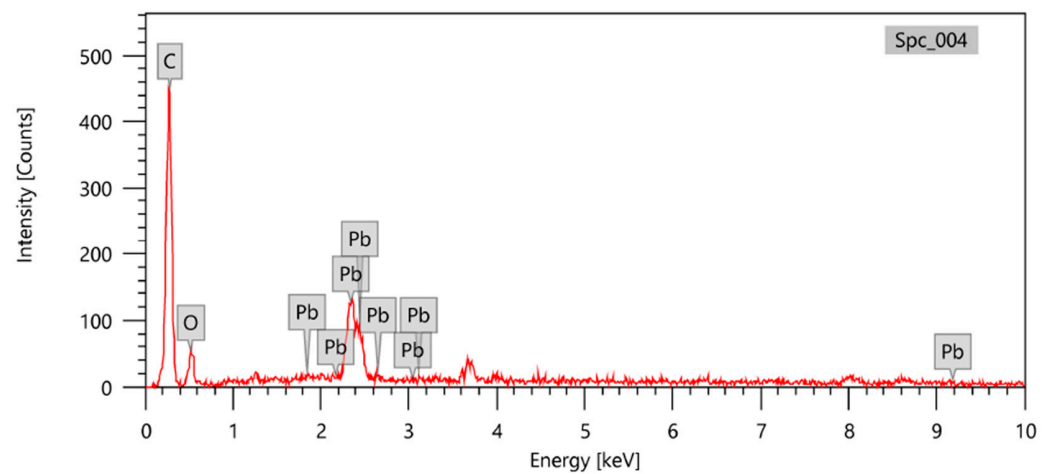


Figure 2. Electron dispersive X-ray (EDX) image of the biochar after Pb(II) adsorption.

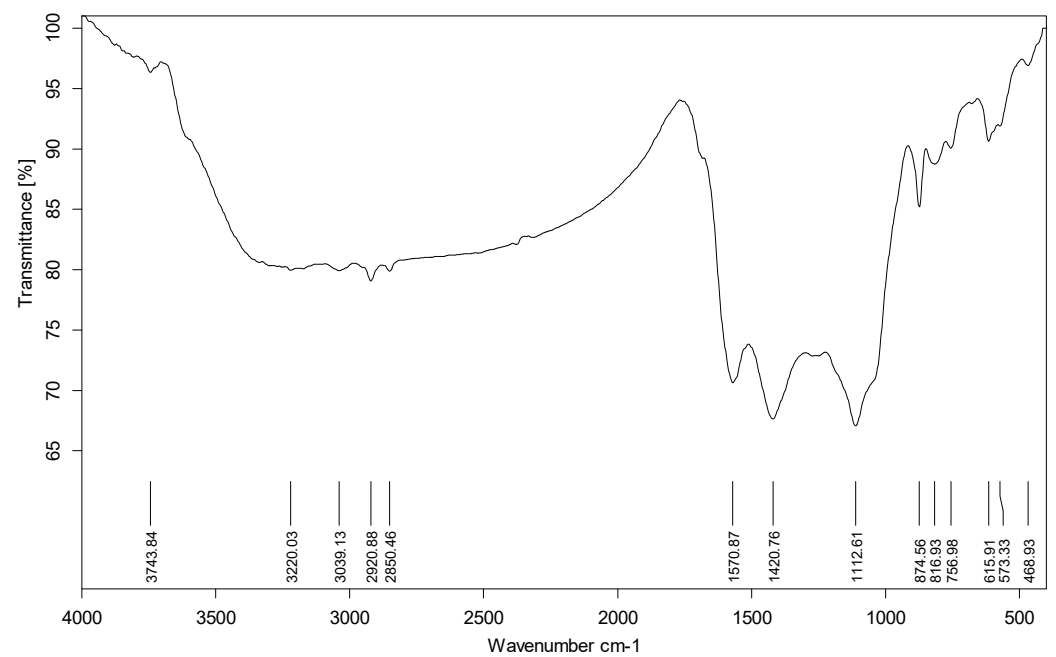


Figure 3. FTIR spectra of biochar before Pb(II) adsorption.

3.2. Adsorption of Pb by Biochar

The study's investigation into the adsorption of Pb(II) by biochar commenced with the calibration of different concentrations of Pb(II) against their corresponding absorbance levels. This relationship, as depicted in Figure 4, was found to be linear, affirming the reliability of the measurements and the method.

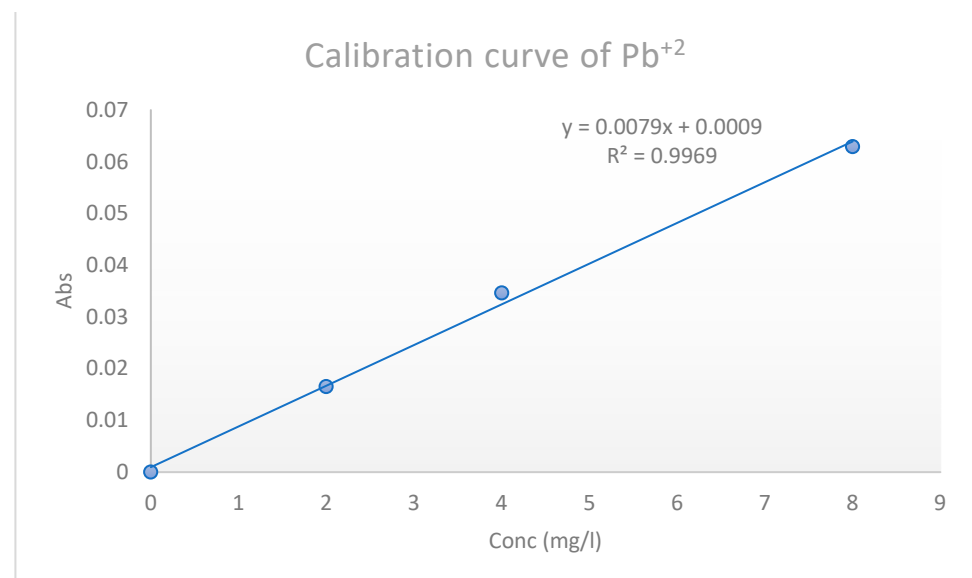


Figure 4. Calibration curve of Pb(II).

To evaluate the biochar's capacity for adsorbing Pb(II), varying amounts were introduced into the aqueous solution. The adsorption percentages of Pb(II) were calculated as outlined in the experimental procedures and are detailed in Table 1. A notable observation from this data is the correlation between increased biochar concentrations and enhanced adsorption of Pb(II). Remarkably, 100% adsorption of Pb(II) was achieved with the addition of 0.06 g/10 mL of biochar. This result highlights the high efficiency of the biochar prepared from the leaf midribs of date palms in removing Pb(II) from aqueous solutions.

Table 1. Adsorption of Pb(II) (100 ppm) on different amounts of biochar.

Amount of Biochar (g/10 mL)	The Mean Concentration of Pb(II) (mg/L)	% of Adsorption
0	100	0
0.02	0.15	99.85
0.04	0.11	99.89
0.06	0	100
0.08	0	100

Several mechanisms are likely contributing to this high level of Pb(II) removal, including precipitation, complexation, ion exchange, electrostatic attraction, chemical bond adsorption, and physical adsorption. The detection of Pb(II) particles on the biochar surface, attributable to the precipitation of carbonate minerals and phosphates, indicates that precipitation is a significant mechanism in Pb removal [36,37]. Surface complexation also plays a crucial role, where C-O groups on the biochar surface bind with Pb in the solution [38,39]. Notably, the metal complexing ability of hydroxyl groups is generally stronger than that of carboxyl groups [40].

Ion exchange processes involving the cations on the oxygen-containing functional groups and Pb ions also contribute to Pb removal [41]. Electrostatic interactions enable Pb to combine with -COOH and -OH groups on the biochar [42]. Additionally, the effect of pH on Pb ion precipitation is significant. At pH levels above 6.0, local sites of high alkalinity on the biochar surface led to further precipitation [43,44]. Furthermore, an increase in pyrolysis temperature has been noted to enhance the effect of mineral precipitation.

This comprehensive analysis of the Pb(II) adsorption process by the date palm-derived biochar demonstrates its potential as an effective and sustainable solution for lead removal in water treatment applications. The variety of mechanisms at play highlights the multifaceted nature of biochar as an adsorbent and its suitability for addressing heavy metal contamination in environmental settings.

As described by Pam Aloysius Akaangee [45], the conventional methods used for the removal of Pb(II) from aqueous solutions have limitations and side effects. Therefore, adsorption onto solid adsorbents, especially activated carbon, is an excellent method that can be used for the adsorption of Pb(II) from aqueous solutions. This is due to the high efficiency of adsorption and sorption capacities. In the work of Aloysius [45], activated carbon (AC) was prepared by the chemical treatment of palm kernel shells (PKS) using H_3PO_4 and later modified using citric acid (CA) and ethylenediaminetetraacetic acid (EDTA). The maximum adsorption capacity of Pb(II) was in the sequence of ACPKS (86.2 mg/g) < AC-CA (103.1 mg/g) < AC-EDTA (104.2 mg/g). However, the cost of these methods is higher than that of the biochar prepared in the present work.

In another study by Saud S. Aloud et al. [46], activated carbon was produced from the leaf sheath fibers of date palms (LSDPFAC) by the use of chemical activation with K_2CO_3 combined with microwave irradiation, and it was characterized and evaluated for its adsorptive capacity of lead ions (Pb(II)). A greater adsorption of Pb(II) was observed when its concentration was higher in the solution, and the greatest adsorption capacity of 5.67 mg Pb/g was observed at the highest pH.

3.3. Adsorption of Iodine by Biochar

In assessing the biochar's capacity for iodine adsorption, we explored how different quantities of biochar influenced the removal process. This experiment involved adding varying amounts of biochar (0.1, 0.2, 0.3, and 0.4 g/50 mL) to an iodine solution, with the outcomes detailed in Table 2. Notably, the biochar demonstrated a maximum adsorption percentage of 39.7% when 0.3 or 0.4 g/50 mL was used. This finding, as highlighted in

the table, is crucial as it indicates the threshold beyond which additional biochar does not significantly increase adsorption efficiency.

Table 2. Adsorption of iodine on different amounts of biochar.

Amount of Biochar (g/50 mL)	% of Adsorption
0.1	24.1
0.2	27.7
0.3	33.7
0.4	39.7

To delve deeper into the adsorption dynamics, we extended our investigation to the impact of incubation time. Figure 5 illustrates the variation in iodine adsorption as the incubation period with 0.4 g of biochar was extended from 2 to 30 h. An interesting pattern emerged: extending the incubation time from 2 to 12 h resulted in an increase in adsorption efficiency, from 40% to 60.3%. This increment underscores the importance of sufficient contact time for the adsorption process, allowing for more extensive interaction between iodine molecules and the biochar.

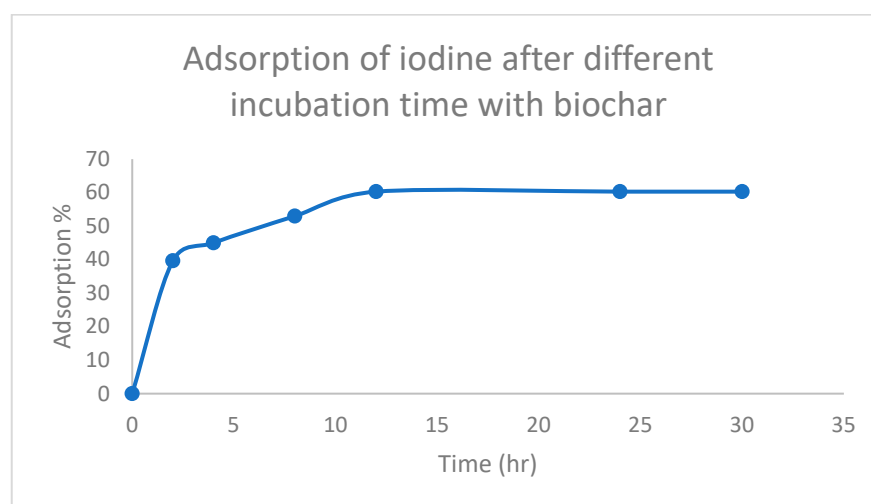


Figure 5. Adsorption of iodine on biochar at different incubation times.

The underlying science of this phenomenon can be attributed to several factors. The elevated pyrolysis temperature used in creating the biochar plays a vital role. It enhances the degree of carbonization, which in turn increases the number of micropores within the biochar [47]. These micropores are key to the adsorption process, providing sites where iodine molecules can be trapped. However, after a 12 h period, we observed a plateau in adsorption efficiency. This suggests that beyond this point, all readily accessible adsorption sites on the biochar were occupied, and additional contact time did not contribute to further iodine removal.

The adsorption efficiency of iodine on biochar at various pH levels was systematically studied to understand how pH influences the removal process. The results, presented in Table 3, indicate that pH plays a significant role in the adsorption capacity of biochar for iodine. At a pH of 2, the adsorption percentage was recorded at 24.1%. This relatively low adsorption efficiency can be attributed to the high concentration of hydrogen ions (H^+) in the solution at this pH level, which compete with iodine ions for active sites on the biochar surface. As the pH increases to 3, the adsorption efficiency improves to 27.7%, indicating a reduction in competitive adsorption by hydrogen ions and an increase in the availability of active sites for iodine ions. Further increasing the pH to 4 results in a more

pronounced improvement in adsorption efficiency, reaching 33.7%. This trend continues as the pH rises to 5, where the adsorption percentage increases to 39.5%. The increase in adsorption capacity with rising pH can be attributed to the deprotonation of functional groups on the biochar surface, such as carboxyl and hydroxyl groups, which enhance their interaction with iodine ions. At a pH of 6, the adsorption efficiency reaches a maximum of 39.7%. This slight increase from pH 5 to pH 6 suggests that the adsorption process stabilizes, and the biochar surface becomes fully saturated with iodine ions. The relatively constant adsorption efficiency at higher pH levels indicates that the biochar's active sites are fully utilized, and further increases in pH would not significantly enhance the adsorption capacity. The results illustrate that the adsorption of iodine on biochar is highly dependent on the pH of the solution. The optimal pH for maximum iodine adsorption was found to be around 6, where the biochar achieved an adsorption efficiency of 39.7%. These findings suggest that adjusting the pH of the solution can be an effective strategy to enhance the removal efficiency of iodine using biochar, thereby optimizing the treatment process for contaminated water.

Table 3. Adsorption of iodine at different pH.

pH	% Adsorption
2	24.1
3	27.7
4	33.7
5	39.5
6	39.7

The effect of the initial iodine concentration on the adsorption efficiency of biochar was investigated to determine the optimal conditions for maximum iodine removal from aqueous solutions. The results, presented in Table 4, indicate a clear trend in the adsorption capacity as a function of initial iodine concentration. At an initial iodine concentration of 20 mg/L, the biochar demonstrated an adsorption efficiency of 55.4%. This high percentage can be attributed to the ample availability of active adsorption sites on the biochar surface relative to the number of iodine ions present. As the initial concentration increases to 40 mg/L, the adsorption efficiency slightly decreases to 50%. This reduction suggests that as the concentration of iodine ions increases, the available active sites on the biochar become more occupied, leading to increased competition among iodine ions for the remaining active sites. Further increasing the initial concentration to 60 mg/L results in a continued decrease in adsorption efficiency to 47.1%. This trend persists with initial concentrations of 80 mg/L and 100 mg/L, where the adsorption efficiencies are 43.4% and 39.7%, respectively. The decrease in adsorption efficiency with increasing initial iodine concentration can be explained by the saturation of active sites on the biochar surface. As more iodine ions are introduced into the solution, the biochar's active sites become fully occupied, reducing the overall adsorption capacity. The results suggest that at lower initial concentrations, biochar exhibits higher adsorption efficiencies due to the greater availability of active sites. However, as the initial iodine concentration increases, the adsorption efficiency declines, indicating a limitation in the biochar's capacity to adsorb higher concentrations of iodine. This behavior is typical in adsorption processes, where the adsorbent's capacity is finite, and higher concentrations of the adsorbate lead to reduced efficiency. The results demonstrate that the initial concentration of iodine significantly affects the adsorption efficiency of biochar. The optimal adsorption efficiency was observed at an initial concentration of 20 mg/L, with a value of 55.4%. As the initial concentration increases, the adsorption efficiency decreases, reaching 39.7% at an initial concentration of 100 mg/L. These findings highlight the importance of considering initial iodine concentration when optimizing biochar for water treatment applications, ensuring that the biochar is used effectively to maximize contaminant removal.

Table 4. Effect of initial concentration of iodine.

Initial Concentration (mg/L)	% Adsorption
20	55.4
40	50
60	47.1
80	43.4
100	39.7

The physical and chemical characteristics of the biochar, such as surface area and pore structure, greatly influence its adsorption capacity. Iodine molecules are primarily adsorbed into micropores on the biochar [48–50], and the extent of these micropores, typically less than 2 nm in size, correlates with the biochar’s iodine index [51]. It is noteworthy that the adsorption percentages for iodine are lower compared to Pb(II), which can be attributed to the differences in the adsorption mechanisms and the inherent properties of the adsorbents and adsorbates.

In the broader context of adsorbent materials, biochar generally shows a lower iodine adsorption capacity than activated charcoal [52]. This difference is largely due to variations in pore formation, which are significantly influenced by the activation temperature during the production of activated carbon [53].

An additional factor in iodine adsorption is the iodine number, a measure of the adsorbent’s capacity to adsorb iodine. This value can be affected by impurities on the biochar surface that chemically react with iodine [54,55]. For instance, high levels of oxygen complexes, such as carboxyl groups on the biochar, may reduce the iodine number due to their reaction with potassium iodine [56].

In conclusion, this in-depth analysis of iodine adsorption on biochar sheds light on the complex interplay of factors that determine the efficiency of the adsorption process. The findings not only highlight the biochar’s capacity for iodine removal but also provide insights into optimizing the use of biochar in environmental remediation, particularly for iodine and, potentially, other similar contaminants.

4. Conclusions

This study has successfully demonstrated the adsorption of Pb(II) and iodine from aqueous solutions using biochar derived from the leaf midribs of the date palm through a slow pyrolysis process. The experimental approach involved incubating a 100 ppm Pb(II) ion solution with varying amounts of biochar (20, 40, 60, and 80 mg) for 24 h. Similarly, for iodine adsorption, different amounts of biochar (0.1, 0.2, 0.3, and 0.4 g) were incubated with a 50 mL solution of 0.1 M iodine. The concentrations of Pb(II) and iodine remaining in the solutions post-treatment were accurately quantified using atomic absorption spectroscopy.

The key conclusions drawn from this research are as follows:

Biochar Structure and Functional Groups: The biochar produced exhibited a porous structure with lateral and anterior vessels, characterized by large numbers of pores measuring approximately 20 to 50 μm . Additionally, functional groups vital to adsorption processes, such as O-H, C-H, and ring-stretching C=C groups, were identified in the biochar. This structure and composition were directly attributable to the slow pyrolysis of the date palm leaf midribs.

Effective Pb(II) Adsorption: Remarkably, the study achieved 100% adsorption efficiency for Pb(II) ions using just 0.06 g of biochar per 10 mL of the prepared solution. This result highlights the biochar’s exceptional capacity for heavy metal ion removal, positioning it as a viable option for water purification applications.

Iodine Adsorption Capacity: For iodine, the biochar demonstrated a maximum adsorption percentage of 39.7% when used in quantities of 0.3 or 0.4 g per 50 mL of the solution. This finding suggests that while biochar is effective in adsorbing iodine, the

adsorption capacity is comparatively lower than that for Pb(II), likely due to differences in the adsorption mechanisms and the inherent properties of iodine.

These conclusions underscore the potential of date palm-derived biochar as a sustainable and efficient material for the adsorption of contaminants like Pb(II) and iodine from aqueous solutions. The study not only provides a promising method for environmental remediation but also offers insights into optimizing biochar production for specific adsorption applications. Given the promising results of this research, it is recommended to conduct a subsequent and more detailed study focusing on the effects of various heavy metals. Additionally, the subsequent study should delve into kinetics, isotherms, and thermodynamic analysis.

Author Contributions: Conceptualization, E.R.I.M. and H.M.A.; methodology, H.M.A. and H.F.E.-L.; validation, E.R.I.M., H.M.A. and N.A.H.; formal analysis, H.M.A.; investigation, N.A.H.; resources, N.A.H.; data curation, H.F.E.-L.; writing—review and editing, H.F.E.-L. and A.L.K.; visualization, H.M.A. and A.A.; supervision, A.L.K.; project administration, A.A.; funding acquisition, E.R.I.M. All authors have read and agreed to the published version of the manuscript.

Funding: This research received no external funding.

Data Availability Statement: The data will be available on request.

Acknowledgments: The authors would like to express their appreciation for the support provided by the Scientific Research Deanship, Islamic University of Madinah.

Conflicts of Interest: The authors declare no conflicts of interest.

References

1. Wang, C.; Wang, X.; Li, N.; Tao, J.; Yan, B.; Cui, X.; Chen, G. Adsorption of Lead from Aqueous Solution by Biochar: A Review. *Clean Technol.* **2022**, *4*, 629–652. Available online: <https://www.mdpi.com/journal/cleantechnol> (accessed on 26 May 2024). [[CrossRef](#)]
2. Naseem, R.; Tahir, S.S. Removal of Pb (II) from aqueous/acidic solutions by using bentonite as an adsorbent. *Water Res.* **2001**, *35*, 3982–3986. [[CrossRef](#)] [[PubMed](#)]
3. Campos, P.; De la Rosa, J.M. Assessing the Effects of Biochar on the Immobilization of Trace Elements and Plant Development in a Naturally Contaminated Soil. *Sustainability* **2020**, *12*, 6025. Available online: www.mdpi.com/journal/sustainability (accessed on 26 May 2024). [[CrossRef](#)]
4. Zhao, J.J.; Shen, X.-J.; Domene, X.; Alcañiz, J.-M.; Liao, X.; Palet, C. Comparison of biochars derived from different types of feedstock and their potential for heavy metal removal in multiple-metal solutions. *Sci. Rep.* **2019**, *9*, 9869. [[CrossRef](#)] [[PubMed](#)]
5. Campos, P.; Miller, A.Z.; Knicker, H.; Costa-Pereira, M.F.; Merino, A.; De la Rosa, J.M. Chemical, physical and morphological properties of biochars produced from agricultural residues: Implications for their use as soil amendment. *J. Waste Manag.* **2020**, *105*, 256–267. [[CrossRef](#)] [[PubMed](#)]
6. Liu, Z.G.; Zhang, F.S. Removal of lead from water using biochars prepared from hydrothermal liquefaction of biomass. *J. Hazard. Mater.* **2009**, *167*, 933–939. [[CrossRef](#)] [[PubMed](#)]
7. Tahir, A.H.F.; Al-Obaidy, A.H.M.J.; Mohammed, F.H. Biochar from date palm waste, production, characteristics and use in the treatment of pollutants: A Review. *IOP Conf. Ser. Mater. Sci. Eng.* **2020**, *737*, 012171. [[CrossRef](#)]
8. Ghanim, A.N. Utilization of date pits derived bio-adsorbent for heavy metals in wastewater treatment: Review. *Al-Qadisiyah J. Eng. Sci.* **2023**, *16*, 058–069. [[CrossRef](#)]
9. Alghamdi, A.G.; Alasmary, Z. Efficient Remediation of Cadmium- and Lead-Contaminated Water by Using Fe-Modified Date Palm Waste Biochar-Based Adsorbents. *Int. J. Environ. Res. Public Health* **2023**, *20*, 802. [[CrossRef](#)] [[PubMed](#)]
10. Thabeta, W.M.; Ahmedb, S.B.; Abdelwahaba, O.; Soliman, N.F. Enhancement Adsorption of Lead and Cadmium Ions from Waste Solutions Using Chemically Modified Palm fibers. *Egypt. J. Chem.* **2020**, *63*, 4917–4927. [[CrossRef](#)]
11. Mahdi, Z.; Yu, Q.J.; El Hanandeh, A. Removal of lead(II) from aqueous solution using date seed-derived biochar: Batch and column studies. *Appl. Water Sci.* **2018**, *8*, 181. [[CrossRef](#)]
12. Zare, L.; Ghasemi-Fasaei, R. Investigation of Equilibrium Isotherm and Kinetic Modeling to Assess Sorption Characteristics of Nitrate onto Palm Leaf Biochar. *Iran. J. Chem. Chem. Eng.* **2019**, *38*, 5.
13. Barman, B.K.; Barman, S.; Roy, M.N. Inclusion complexation between tetrabutylphosphonium methanesulfonate as guest and α - and β -cyclodextrin as hosts investigated by physicochemical methodology. *J. Mol. Liq.* **2018**, *264*, 80. [[CrossRef](#)]
14. Wu, Z.; Chen, X.; Yuan, B.; Fu, M.-L. A facile foaming-polymerization strategy to prepare 3D MnO₂ modified biochar-based porous hydrogels for efficient removal of Cd (II) and Pb (II). *Chemosphere* **2019**, *239*, 124745. [[CrossRef](#)] [[PubMed](#)]
15. Lee, X.J.; Lee, L.Y.; Hiew, B.Y.Z.; Gan, S.; Thangalazhy-Gopakumar, S.; Ng, H.K. Multistage optimizations of slow pyrolysis synthesis of biochar from palm oil sludge for adsorption of lead. *Bioresour. Technol.* **2017**, *245*, 944–953. [[CrossRef](#)] [[PubMed](#)]

16. Wang, C.; Wang, H.; Cao, Y. Pb (II) sorption by biochar derived from Cinnamomum camphora and its improvement with ultrasound-assisted alkali activation. *Colloids Surfaces A Physicochem. Eng. Asp.* **2018**, *556*, 177–184. [[CrossRef](#)]
17. Banerjee, D.; Chen, X.; Lobanov, S.S.; Plonka, A.M.X.; Chan Daly, J.A.; Kim, T.; Thallapally, P.K.; Parise, J.B. Iodine adsorption in metal organic frameworks in the presence of humidity. *ACS Appl. Mater. Interfaces* **2018**, *10*, 10622. [[CrossRef](#)] [[PubMed](#)]
18. Abdelmoaty, Y.H.; Tessema, T.D.; Choudhury, F.A.; EL-Kadri, O.M.; EL-Kaderi, H.M. Nitrogen rich porous polymers for carbon dioxide and iodine sequestration for environmental remediation. *ACS Appl. Mater. Interfaces* **2018**, *10*, 16049. [[CrossRef](#)] [[PubMed](#)]
19. Han, W.; Clarke, W.; Pratt, S. Cycling of iodine by microalgae: Iodine uptake and release by a microalgae biofilm in a groundwater-holding pond. *Ecol. Eng.* **2016**, *94*, 286. [[CrossRef](#)]
20. Zhang, T.; Yue, X.; Gao, L.; Qiu, F.; Xu, J.; Rong, J.; Pan, J. Hierarchically porous bismuth oxide/layered double hydroxide composites: Preparation, characterization, and iodine adsorption. *J. Clean. Prod.* **2017**, *144*, 220. [[CrossRef](#)]
21. Zhou, J.; Lan, T.; Li, T.; Chen, Q.; Bai, P.; Liu, F.; Yuan, Z.; Zheng, W.; Luo, X.; Yan, W.; et al. Highly efficient capture of iodine in spent fuel reprocessing offgas by novel porous copper-doped silica zeolites. *Sep. Purif. Technol.* **2022**, *290*, 120895. [[CrossRef](#)]
22. Xie, W.; Cui, D.; Zhang, S.R.; Xu, Y.H.; Jiang, D.L. Iodine capture in porous organic polymers and metal-organic frameworks materials. *Mater. Horiz.* **2016**, *6*, 1571. [[CrossRef](#)]
23. Al-Fulaiti, B.; El-Shafey, E.S.I.; Al Kindi, S.H.S.; Abdel-Jalil, R.J. Adsorption of Iodine from Aqueous Solution on Modified Silica Gel with Cyclodextrin Derivatives. *Pol. J. Environ. Stud.* **2022**, *31*, 5571–5582. [[CrossRef](#)] [[PubMed](#)]
24. Hirota, M.; Higaki, S.; Ito, S.; Ishida, Y.; Terao, K. Effects of 2-hydroxypropyl α -cyclodextrin on the radioactive iodine sorption on activated carbon. *J. Radioanal. Nucl. Chem.* **2021**, *328*, 659. [[CrossRef](#)]
25. Windiastuti, E.; Indrasti, N.S.; Hasanudin, U.; Bindar, Y.; Suprihatin. The Influence of Pretreatment and Post Treatment with Alkaline Activators on the Adsorption Ability of Biochar from Palm Oil Empty Fruit. *J. Ecol. Eng.* **2023**, *24*, 242–251. [[CrossRef](#)]
26. Thoe, J.M.L.; Surugau, N.; Chong, H.L.H. Application of Oil Palm Empty Fruit Bunch as Adsorbent: A Review. *Trans. Sci. Technol.* **2019**, *6*, 9–26.
27. Mahmoud, E.R.I.; Aly, H.M.; Hassan, N.A.; Aljabri, A.; Khan, A.L.; El-Labban, H.F. Biochar from Date Palm Waste via Two-Step Pyrolysis: A Novel Approach for Cu (II) Removal from Wastewater. *Processes* **2024**, *12*, 1189. [[CrossRef](#)]
28. Hergert, H.L. Infrared spectra of lignin and related compounds. II. Conifer lignin and model compounds^{1,2}. *J. Org. Chem.* **1960**, *25*, 405–413. [[CrossRef](#)]
29. Pasieczna-Patkowska, S.; Madej, J. Comparison of photoacoustic, diffuse reflectance attenuated total reflectance and transmission infrared spectroscopy for the study of biochar. *Pol. J. Chem. Technol.* **2018**, *20*, 75–83. [[CrossRef](#)]
30. Abdulrazzaq, H.; Jol, H.; Husni, A. Biochar from Empty Fruit Bunches, Wood, and Rice Husks: Effects on Soil Physical Properties and Growth of Sweet Corn on Acidic Soil. *J. Agric. Sci.* **2015**, *7*, 192–200. Available online: www.ccsenet.org/jas (accessed on 26 May 2024). [[CrossRef](#)]
31. Cantrell, K.B.; Hunt, P.G.; Uchimiya, M.; Novak, J.M.; Ro, K.S. Impact of pyrolysis temperature and manure source on physico-chemical characteristics of biochar. *Bioresour. Technol.* **2012**, *107*, 419–428. [[CrossRef](#)] [[PubMed](#)]
32. Saelee, K.; Yingkamhaeng, N.; Nimchua, T.; Sukyai, P. The 6 Extraction and Characterization of cellulose from sugarcane bagasse by using environmental friendly method. In Proceedings of the 26th Annual Meeting of the Thai Society for Biotechnology and International Conference, Chiang Rai, Thailand, 26–29 November 2014.
33. Prapagdee, S.; Piyatiratitvorakul, S.; Petsom, A.; Tawinteung, N. Application of biochar for enhancing cadmium and zinc phytostabilization in *Vigna radiata* L. cultivation. *Water Air Soil Pollut.* **2014**, *225*, 2233. [[CrossRef](#)]
34. Tong, X.U.E.; Ren-Qing, W.; Zhang, M.-M.; Jiu-Lan, D.A.I. Adsorption and desorption of mercury (II) in three forest soils in Shandong Province, China. *Pedosphere* **2013**, *23*, 265–272.
35. Keiluweit, M.; Nico, P.S.; Johnson, M.G.; Kleber, M. Dynamic molecular structure of plant biomass-derived black carbon (biochar). *Environ. Sci. Technol.* **2010**, *44*, 1247–1253. [[CrossRef](#)] [[PubMed](#)]
36. Chang, J.; Zhang, H.; Cheng, H.; Yan, Y.; Chang, M.; Cao, Y.; Huang, F.; Zhang, G.; Yan, M. Spent Ganoderma lucidum substrate derived biochar as a new bio-adsorbent for Pb²⁺/Cd²⁺ removal in water. *Chemosphere* **2020**, *241*, 125121. [[CrossRef](#)] [[PubMed](#)]
37. Yang, Z.; Hou, J.; Wu, J.; Miao, L. The effect of carbonization temperature on the capacity and mechanisms of Pb (II) adsorption by microalgae residue-derived biochar. *Ecotoxicol. Environ. Saf.* **2021**, *225*, 112750. [[CrossRef](#)] [[PubMed](#)]
38. Cheng, S.; Liu, Y.; Xing, B.; Qin, X.; Zhang, C.; Xia, H. Lead and cadmium clean removal from wastewater by sustainable biochar derived from poplar saw dust. *J. Clean. Prod.* **2021**, *314*, 128074. [[CrossRef](#)]
39. Gao, R.; Xiang, L.; Hu, H.; Fu, Q.; Zhu, J.; Liu, Y.; Huang, G. High-efficiency removal capacities and quantitative sorption mechanisms of Pb by oxidized rape straw biochars. *Sci. Total Environ.* **2019**, *699*, 134262. [[CrossRef](#)] [[PubMed](#)]
40. Zhao, M.; Dai, Y.; Zhang, M.; Feng, C.; Qin, B.; Zhang, W.; Zhao, N.; Li, Y.; Ni, Z.; Xu, Z.; et al. Mechanisms of Pb and/or Zn adsorption by different biochars: Biochar characteristics, stability, and binding energies. *Sci. Total Environ.* **2020**, *717*, 136894. [[CrossRef](#)] [[PubMed](#)]
41. Yang, X.; Wan, Y.; Zheng, Y.; He, F.; Yu, Z.; Huang, J.; Wang, H.; Ok, Y.S.; Jiang, Y.; Gao, B. Surface functional groups of carbon-based adsorbents and their roles in the removal of heavy metals from aqueous solutions: A critical review. *Chem. Eng. J.* **2019**, *366*, 608–621. [[CrossRef](#)] [[PubMed](#)]
42. Zhao, T.; Yao, Y.; Li, D.; Wu, F.; Zhang, C.; Gao, B. Facile low-temperature one-step synthesis of pomelo peel biochar under air atmosphere and its adsorption behaviors for Ag (I) and Pb (II). *Sci. Total Environ.* **2018**, *640–641*, 73–79. [[CrossRef](#)] [[PubMed](#)]

43. Mohan, D.; Singh, P.; Sarswat, A.; Steele, P.H.; Pittman, C.U., Jr. Lead sorptive removal using magnetic and nonmagnetic fast pyrolysis energy cane biochars. *J. Colloid Interface Sci.* **2015**, *448*, 238–250. [[CrossRef](#)] [[PubMed](#)]
44. Shi, J.; Fan, X.; Tsang, D.C.; Wang, F.; Shen, Z.; Hou, D.; Alessi, D.S. Removal of lead by rice husk biochars produced at different temperatures and implications for their environmental utilizations. *Chemosphere* **2019**, *235*, 825–831. [[CrossRef](#)] [[PubMed](#)]
45. Aloysius, A.P. Adsorption of Lead from Aqueous Solution using Modified Activated Carbon prepared from Palm Kernel Shell. Ph.D. Thesis, Universiti Putra Malaysia, Serdang, Malaysia, March 2018.
46. Aloud, S.S.; Hameed, B.H.; Yusop, M.F.M.; Alharbi, H.A.; Giesy, J.P.; Alotaibi, K.D. Adsorption of Pb²⁺ by Activated Carbon Produced by Microwave-Assisted K₂CO₃ Activation of Date Palm Leaf Sheath Fibres. *Water* **2023**, *15*, 3905. [[CrossRef](#)]
47. Powar, R.V.; Gangil, S. Effect of temperature on iodine value and total carbon contain in biochar produced from soybean stalk in continuous feed reactor. *J. Agric. Eng.* **2015**, *8*, 26–30. [[CrossRef](#)]
48. Yenisoym-Karakas, S.; Aygün, A.; Günes, M.; Tahtasakal, E. Physical and chemical characteristics of polymerbased spherical activated carbon and its ability to adsorb organics. *Carbon* **2004**, *42*, 477–484. [[CrossRef](#)]
49. Hernandez-Maglinao, J.; Capareda, S.C. Improving the Surface Areas and Pore Volumes of Biochar Produced from Pyrolysis of Cotton Gin Trash via Steam Activation Process. *Int. J. Eng. Sci.* **2019**, *3*, 15–18.
50. Saleh, M.E.; Mahmoud, A.H.; Rashad, M. April Biochar usage as a cost-effective bio-sorbent for removing NH₄-N from wastewater. In Proceedings of the International Conference the Global Climate Change, Biodiversity and Sustainability: Challenges and Opportunities—An International Conference Focused on the Arab MENA Region and EuroMed, Alexandria, Egypt, 15–18 April 2013; pp. 15–18.
51. Castiglioni, M.; Rivoira, L.; Ingrand, I.; Del Bubba, M.; Bruzzoniti, M.C. Characterization Techniques as Supporting Tools for the Interpretation of Biochar Adsorption Efficiency in Water Treatment: A Critical Review. *Molecules* **2021**, *26*, 5063. [[CrossRef](#)] [[PubMed](#)]
52. Tamrin, K.F.; Zahrim, A.Y. Determination of optimum polymeric coagulant in palm oil mill effluent coagulation using multiple-objective optimisation on the basis of ratio analysis (MOORA). *Environ. Sci. Pollut. Res.* **2017**, *24*, 15863–15869. [[CrossRef](#)] [[PubMed](#)]
53. Jawad, A.H.; Abdulhameed, A.S.; Bahrudin, N.N.; Hum, N.N.M.F.; Surip, S.N.; Syed-Hassan, S.S.A.; Yousif, E.; Sabar, S. Microporous activated carbon developed from KOH activated biomass waste: Surface mechanistic study of methylene blue dye adsorption. *Water Sci. Technol.* **2021**, *84*, 1858–1872. [[CrossRef](#)] [[PubMed](#)]
54. Schroder, A.; Kluppel, M.; Schuster, R.H.; Heidberg, J. Energetic surface heterogeneity of carbon black. *Kautschuk Gummi Kunststoffe* **2001**, *54*, 260–266. Available online: <http://www.plastverarbeiter.de/ai/resources/36a867629d7.pdf> (accessed on 26 May 2024).
55. Wampler, W.A.; Nikiel, L.; Evans, E.N. carbon black. In *Rubber Compounding: Chemistry and Applications*, 2nd ed.; Rodgers, B., Ed.; CRC Press: Boca Raton, FL, USA, 2016; Chapter 6; pp. 209–250.
56. Hess, W.M.; Herd, C.R. Microstructure, morphology, and general physical properties. In *Carbon Black: Science and Technology*, 2nd ed.; Donnet, J.-B., Bansal, R.C., Wang, M.J., Eds.; Marcel Dekker, Inc.: New York, NY, USA, 1993; Chapter 3, pp. 89–174.

Disclaimer/Publisher’s Note: The statements, opinions and data contained in all publications are solely those of the individual author(s) and contributor(s) and not of MDPI and/or the editor(s). MDPI and/or the editor(s) disclaim responsibility for any injury to people or property resulting from any ideas, methods, instructions or products referred to in the content.